Development Of A CFD Model For A CANDU-6 Moderator Analysis Using A Coupled Solver

C. Yoon* **and J. H. Park**
Korea Atomic Energy Research Institute, Daejeon, Korea (ROK)
* Phone: +82-42-868-2128, Fax: +82-42-868-8256, E-mail: cyoon@kaeri.re.kr

Abstract

A CFD moderator analysis model by using a coupled solver has been developed for a CANDU-6 moderator analysis. For Wolsong Units 2/3/4, a steady-state moderator circulation under operating conditions and the local moderator subcooling during a LOCA transient were calculated using the CFD tool. When compared to a former study, the current analysis provided well matched and reasonable results. This new CFD model based on a coupled solver shows a dramatic increase in the computing speed, when compared to that based on a segregated solver.

1. Introduction

When a PHT(Primary Heat Transfer) system fails to remove excess heat from fuel channels for some loss of coolant accidents(LOCA's) of CANDU NPP's, the fuel channel temperature could increase until the pressure tube strains (i.e., balloon or sag) to contact its surrounding Calandria tube.(PT/CT contact) Following a PT/CT contact, there is a spike in the heat flux to the moderator surrounding the Calandria tube, which may lead to a sustained CT dryout and also a failure of a fuel channel. The prevention of a CT dryout following a PT/CT contact depends on the available local moderator subcooling. That is, fuel channel integrity depends on the capability of the moderator to act as the ultimate heat sink for some LOCA's in a CANDU reactor.

Experimental studies on the moderator circulation and temperature distribution have been underway in Canada since the early 80's. Austman et al.[1] measured the moderator temperature by inserting thermal-couples through a SOR Guide tube in operating CANDU reactors, of Bruce A and Pickering. Huget et al.[2,3] conducted 2-dimensional moderator circulation tests at a 1/4-scaled facility in the STERN Lab. From those researches, the existence of three clearly distinct flow patterns was observed according to certain *Archimedes* number ranges. Khartabil et al.[4] reported that 3-dimensional moderator circulation tests had been conducted at Chalk River Lab. along with separate phenomena tests related to a CANDU moderator circulation such as a hydraulic resistance through tube bundles, velocity profiles at an inlet diffuser, flow development along a curved wall, and turbulence generation by temperature differences. Based on these experimental works, a CFD code for a CANDU moderator analysis, MODTURC_CLAS, has been developed and selected by the Canadian industry as its standard tool. This CFD tool is being used for the design of ACR and CANDU as well as the CANDU safety analysis.

In KAERI, Yoon et al.[5] developed a CFD model for predicting a CANDU-6 moderator temperature on the basis of a commercial CFD code CFX-4(ANSYS Inc.). This analytic model has some strength in the modelling of hydraulic resistances in the core region and in the treatment of a heat source term in the energy equations. But convergence difficulties and a slow computing speed are the limitations of this model, because the CFX-4 code adapts a segregated solver to resolve a moderator circulation including a strong coupled-effect.

Compared to a segregated solver, a coupled-solver is highly efficient and robust especially for a flow with a strong interference between the variables such as combustion. In this study, the developed moderator analysis model based on CFX-4 is transformed into a new moderator analysis model based on CFX-10(ANSYS Inc.) that adapts a coupled solver. The new model is examined and the results are compared with the former results. For Wolsong Units 2/3/4, a steady-state moderator circulation under operating conditions and a local moderator subcooling during a LOCA transient were calculated using the developed CFD tool.

2. CFD Modelling

A flow across a single circular cylinder is one of the classical flow problems. A matrix of Calandria tubes is located in the core region. If one wants to simulate a flow through the core region in detail, they might require quite a large number of cells more than hundreds of thousands per tube and consequently a huge computing time. Therefore, by discarding the detailed phenomena of the interaction between the tube surfaces and the fluid flows such as a laminar separation and vortex shedding, the tube matrix in the core region is conventionally approximated as a porous medium. With the volume porosity γ and the area porosity γ_A, the governing equations of an incompressible and single-phase liquid flow in the core region are as follows.

$$\frac{\partial(\rho\gamma)}{\partial t}+\frac{\partial\left(\rho\gamma_A u_j\right)}{\partial x_j}=0 \tag{1}$$

$$\frac{\partial(\rho\gamma u_i)}{\partial t}+\frac{\partial\left(\rho\gamma_A u_j u_i\right)}{\partial x_j}=-\gamma_A\frac{\partial p}{\partial x_i}+\frac{\partial}{\partial x_j}\left[\mu_e\gamma_A\left(\frac{\partial u_i}{\partial x_j}+\frac{\partial u_j}{\partial x_i}\right)\right]+B-R \tag{2}$$

$$\frac{\partial(\rho\gamma H)}{\partial t}+\frac{\partial\left(\rho\gamma_A u_j H\right)}{\partial x_j}=\frac{\partial}{\partial x_j}\left(\Gamma_e\gamma_A\frac{\partial H}{\partial x_j}\right)+\gamma Q \tag{3}$$

Equations (1) ~ (3) become the general governing equations with $\gamma=1$. CFX-10[6] uses an un-staggered, collocated grid. To overcome the decoupling (checkerboard) problem of the pressure and velocity components, the continuity equation is rearranged as

$$\left(\frac{\partial u}{\partial x}\right)_i+\frac{\Delta x^3 A}{4\dot{m}}\left(\frac{\partial^4 p}{\partial x^4}\right)_i=0\ . \tag{4}$$

Here, $\dot{m} = \rho u_j \Delta n_j$. As the grid spacing reduces, the second term becomes to zero at a rate of Δx^3 and eq. (4) becomes the general continuity equation.

The standard k-ε turbulence model associated with a logarithmic wall treatment is used to model the turbulence generation and dissipation within the vessel. Buoyancy forces are modeled as a source term in the momentum equations by using the Boussinesq approximation, in which the density is assumed to be a linear function of the temperature.

The fluid flow passing through porous medium is accelerated due to a passage contraction and decelerated due to a flow resistance, coincidently. Because the flow acceleration concerns the area of a fluid passage, it is only determined by using its porosities. The flow resistance consists of a form drag and a frictional pressure loss, which are strongly dependent on the shape and the distributing pattern of any obstacles as well as the flow characteristics. Thus, the resistance source term *R* in equation (2) should be implemented carefully with empirical correlations.

To express the hydraulic resistance of a 3-dimensional velocity vector, a 3-dimensional pressure drop per unit travelling length is expressed in the form of

$$\frac{\Delta p}{\Delta L} = \left.\frac{\Delta p}{\Delta L}\right)_{\substack{cross\\flow}} \cdot \left({S_V}/{S_{90}} \right) \tag{5}$$

For the transverse (lateral) flow across the tube bank, Hadaller et al. [7] investigated the pressure drop of the fluid flows crossing staggered and in-line tube banks, in which the tube Reynolds number range was 2,000 to 9,000 and the pitch-to-diameter ratio was 2.16. The obtained empirical correlation for the pressure loss coefficient is expressed below, regardless of the tube array configuration (staggered or in-line).

$$\left.\frac{\Delta P}{\Delta L}\right)_{\substack{cross\\flow}} = \frac{4.54\,\gamma^2}{pitch} \mathrm{Re}_{tube}^{-0.172} \frac{\rho U}{2} u_i \tag{6}$$

Now, $\left({S_V}/{S_{90}} \right)$ is a ratio of the pressure loss through inclined tube banks to the cross flow pressure loss, which is determined by empirical correlations. Khartabil et al. [4] measured the flow resistance in a test apparatus with inclined tube banks at three different attack angles (30^o, 60^o, & 90^o) for a Reynolds number range of 5,000 to 50,000.

2.1 Verification of the hydraulic resistance terms

Predicted pressure drops of the fluid flow in a rectangular channel containing a porous media blockage are compared with the experimental data by Hadaller et al. [7], for a verification of the hydraulic resistance implementation in CFX-10. Figure 1(a) shows the experimental setup for measuring the pressure losses across transverse tube bundles, and Fig. 1(b) shows the computational domain using the porous media approaches. The rectangular channel of the experimental test section has a cross section of 0.2856 m (Width) x 0.2 m (Height), and is 2 mlong. The tube diameter is 0.03302 meter, and the pitch is 0.0714 meter. Thus, the porosity of the assumed porous media is 0.832.

From Table 1, we can see that the pressure losses predicted by CFX10 are considerably well matched with other simulation results and the measured pressure drop. We can conclude that the isotropic pressure loss model for the porous domain in CFX-10 is thus verified.

Table 1 Comparison of the simulation results against the STERN Lab. Experiments

		STERN T.P. 326	STERN T.P. 299	STERN T.P. 306
Tube Reynolds No.		2746	5237	9392
*ΔP [Pa]	Measurement	28.2	41.3	78.7
	CFX-4	28.8	41.7	80.13
	MODTURC [7]	30.5	44.9	87.3
	CFX-10	27.8	41.6	80.1

* P is the pressure differences between the Pressure Tap 1 (0.5002 m from inlet) and the Pressure Tap 3 (1.6526 m from inlet).

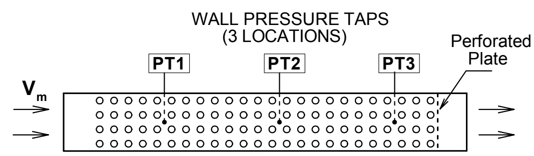

(a) Experimental setup

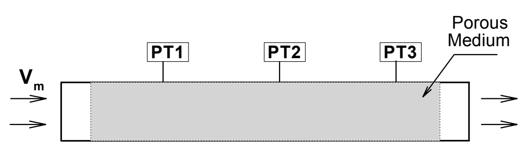

(b) Computational domain for verification

Figure 1 Test apparatus and computational domain

2.2 Validation of the CFD model

Validation is a procedure to test the extent to which the model accurately represents a reality. The small scale CANDU moderator experiments of the Stern Laboratories Inc.(SLI) by Huget et al.[2,3] are used for a validation. The moderator test vessel is a cylinder with a diameter of 2 m and a length of 0.2 m. The vessel does not have a scaled geometry from actual CANDU reactors and is rather close to a thin axial slice of a CANDU-6 Calandria vessel. The experimental data used for a validation in this study is classified as a nominal-conditions test with a flow rate of 2.4 kg/s and a heat load of 100 kW. The inlet temperature is maintained at 55°C for the nominal-conditions test.

The predicted velocity field and temperature distribution by using CFX-10 is presented in Fig. 3. The flow pattern of a nominal-condition test is found to be a ‘mixed-type’ (or non-symmetric jet-momentum-dominated flow pattern). In the results of a nominal-condition prediction, a flow reversal is only observed at one side. The cold injected fluid from the other side's inlet nozzle goes all the way through the upper reflector region, guided by the upper circumferential vessel wall. The two injected fluids meet together at an angle of about 40^{o} over the horizontal centerline, where a jet reversal occurs. The reversed fluid goes down to the bottom, guided by the circumferential lower vessel wall. The velocity vectors in most of the core region are sluggish and skewed upward. The temperature distribution shows a steep change of the temperature around the jet reversal area. The hottest spot is located at the upper center area of the core region, which slightly tilts to one side from the vertical centerline. The maximum temperature calculated by CFX-10 is about 71.4^{o}C, while the measured maximum temperature is 72.4^{o}C.

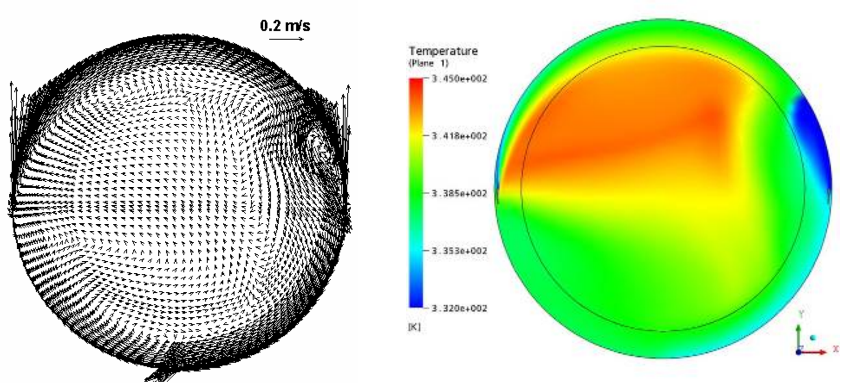

(a) Vector field (b) Temperature

Fig. 2 Velocity field and temperature distribution for the nominal condition of STERN experiments, simulated by CFX-10

3. Steady-State Moderator Circulations

For the moderator analysis of Wolsong NPP Units 2/3/4, the spatial heat distribution of the core region is calculated based on the actual core power map. To reduce the discretization error in the reflector region, butterfly-shaped grid structures (Carlucci et al. [8]) are selected as shown in Fig. 3(a). The butterfly-shaped grid structures allow for finer cells in the reflector region rather than in the core region. This structured hexahedral grid has 113,088 nodes in the core region and 183,696 nodes in the reflector region. The y^+ values at the near wall nodes are in the range of 10 ~ 300.

The steady state computation using CFX-10 was performed in a Pentium IV CPU. The energy imbalances were checked for a convergence. The total CPU time for the RMS residuals to reach a convergence criterion of 10^{-4} was 15 hour 3 min 31 sec, which is about 10 times faster than the case of a segregated solver (CFX-4).

Under normal operating conditions, the calculated maximum temperature of the moderator is 81.1 ^{o}C at the upper center region of the core, which corresponds to a minimum subcooling of 26.5 ^{o}C. Figure 3(b) shows the temperature distributions for normal operating conditions. A jet reversal occurs at an angle of about 50^{o} over the horizontal centerline and the hottest spot is located at the upper center area of the core region, which slightly tilts to one side from the vertical centerline.

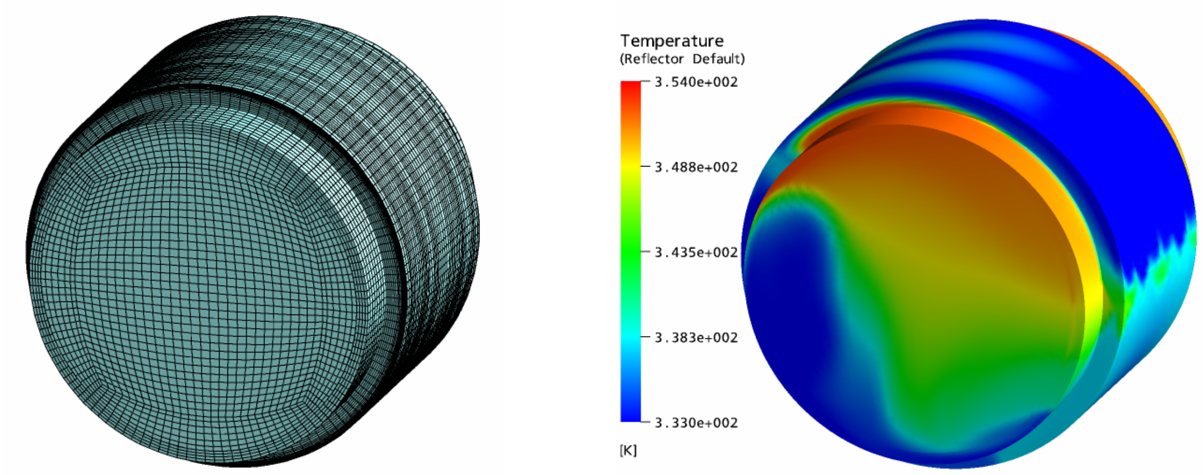

(a) Structured grid structures (b) Steady-state temperature distribution

Fig. 3 Steady-state moderator temperature of the Wolsong Units 2/3/4, simulated by CFX-10

3.1 Effects of the initial conditions

Other remarkable results show that this simulation provided two stable flow circulations. To check the uniqueness of the obtained steady-state condition, a different initial condition is applied. When an initial condition with clock-wise flows in the reflector region was applied, a computational iteration could not overcome the previously formed flow inertia. The alternative steady-state results(Fig. 4(a)) showed a hot spot on the opposite side of the outlet and a jet reversal on the same side as the outlets, which is opposite to that displayed in Fig. 4(b). In this study, it is ensured that an alternative steady circulation condition could be produced depending on the applied initial conditions.

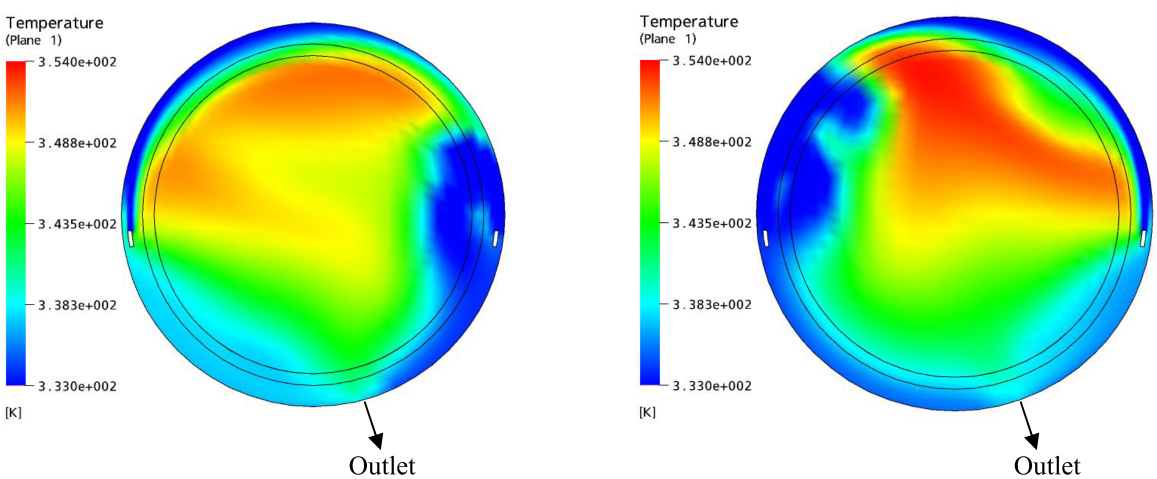

(a) With clock-wise initial flows (b) With zero initial flows

Fig. 4 Comparison of the steady-state temperature distribution at the plane of Z=1.418 m, calculated from different initial conditions

3.2 Local temperature fluctuation

In 1995, M. Collins(1995) reported on the quasi-steady state behaviour of a CANDU-6 moderator circulation by using the PHOENICS2 code. He observed an oscillation of the stagnation point with a period of ~240 sec. To check on this unsteady behaviour under constant operating conditions, a transient computation with a constant condition was performed. The initial condition is the steady-state results. The time step is 0.5 sec and the total time is 930 sec. The RMS residual target for each time step is 10^{-4}.

From the transient calculation results with a constant operating condition, fluctuating temperatures with the time are observed. Figure 5 shows the probing point (X = -2.2, Y = 1.0, Z = 4.582) and the temperature variation during the transient calculation. Especially near the stagnation point, the jet reversal boundaries fluctuate up and down under constant normal operating conditions so that the simulation results show local temperature fluctuations. From several probing locations, the location at (x,y,z) = (-2.2, 1.0, 4.582) shows the largest temperature fluctuation, where the oscillation period is about 14 sec and the fluctuation magnitude is about 6^{o}C. Note that this result is only a qualitative estimation, due to the uncertainties caused by a relatively large time step and grid spacing.

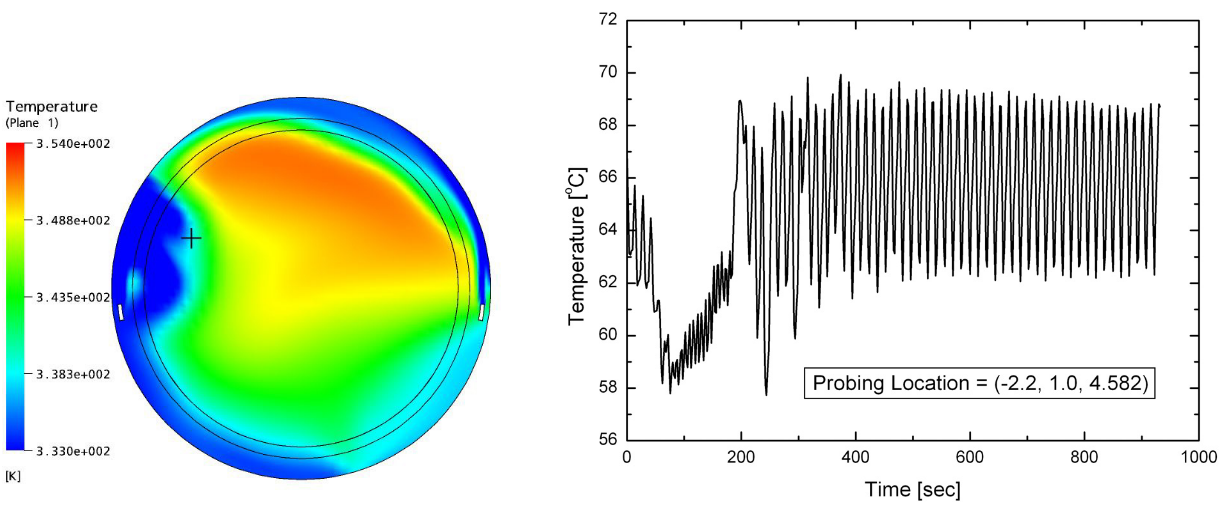

(a) Probing location (-2.2, 1.0, 4.582) (b) Temperature .vs. Time

Figure 5 Temperature variation during the transient calculation under a steady operating condition

3.3 CPU times

To compare the CPU times between the coupled solver and the traditional segregated solver, similar transient simulations for a steady moderator analysis using a segregated solver (ANSYS CFX-4) and a coupled solver (ANSYS CFX-10) are run on HP workstation J6700. Table 2 summarizes the comparison results. The two cases are the same except for using different grids. Coarse meshes with around 40,000 computing nodes are applied and the grid used for the coupled solver has about 17% more cells. Because the solution set of (u, v, w, p) are solved coincidently as one matrix for the coupled 3-dimensional mass-momentum equation set, the size of matrix is much bigger and the CPU time for one (outer) iteration is larger than a traditional segregated solver. But, the required number of outer iterations for a convergence is much smaller in the coupled solver. Therefore, the overall computing speed of the coupled solver is about 5 times faster than the segregated solver when run in the same frame. This table also shows the computing speed of a personal computer with a Pentium IV processor which was faster and used for the current study.

Table 2 Comparison of the CPU times between a segregated solver and a coupled solver

	Segregated solver (CFX-4)	Coupled solver (CFX-10)	
Number of computing nodes	38,272 elements	44,985 nodes	
Machine	HP Visualize J6700 (PA-8700 750MHz processor)	HP Visualize J6700 (PA-8700 750MHz processor)	Personal Computer (Pentium IV 3.2GHz processor)
Time step Δt	0.05 sec	0.05 sec	0.05 sec
Avg. number of (outer) iterations per time step	100	3	4
Avg. CPU time per (outer) iteration	7.89 sec	46.1 sec	13.97 sec
Avg. CPU time per time step	789.0 sec	138.3 sec	69.88 sec

4. Transient Calculations for DBA's

For the transient moderator analysis, the bundle heat load data from multiple single channel analyses by thermal-hydraulic codes such as CATHENA or CHAN should be applied to the source terms of the energy equations. FORTRAN subroutines are written, compiled and linked with the solver. Figure 6 shows the relationship between the solving procedure and the user FORTRAN subroutine. Three user subroutines are used. Firstly, the heat load data is read from the input files and stored. Secondly, the transient time information for each time step is obtained from the solver. And finally, the bundle heat loads to the moderator are implemented into each control volume according to the correspondence between the bundle locations and the vertex coordinates.

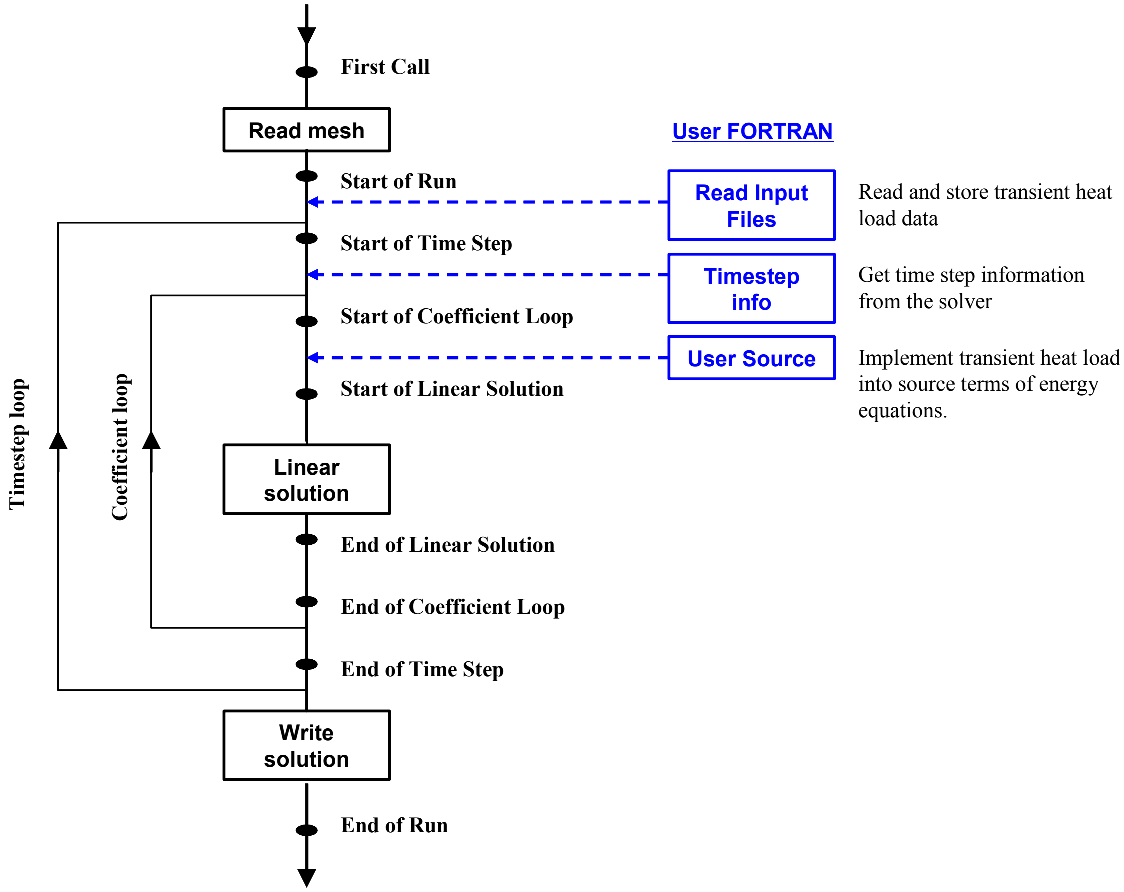

Figure 6 Computation procedure and user FORTRAN subroutines

A 35% RIH(Reactor Inlet Header) break with a loss of ECC(Emergency Core Cooling) injection was selected for the transient analysis, in which the power to the moderator following a PT/CT contact is higher than other LOCA's with a LOECC. The direct heating rate by the gamma-ray from the fission products decreases exponentially ("B" in Fig. 7), and the spatial distribution of a direct heating is assumed to follow the operating power distribution. The PT/CT contact heat transfer("A" in Fig. 7) occurs at various locations at different times according to the results of the fuel channel analyses by CATHENA and CHAN-IIA.

The moderator heat load curve has three distinct humps, which are due to the LOCA power pulse(~1 sec), the PT/CT contacts of the critical pass during the Blowdown Phase(0~40 sec), and the PT/CT contacts of the broken loop during the Post-Blowdown Phase(after 40 sec). The overall moderator temperature hardly changes during the LOCA power pulse at about 1 sec, due to a relatively short time period. Due to PT/CT contacts, the flow field and the temperature distribution after 20 sec experiences some local changes. However, the flow pattern remains about the same as the steady-state flow pattern.

Figure 8 is a plot of a local minimum subcooling of the horizontal plane at a depth of the 5 selected channel rows. The local subcooling at the depths of the A and D rows of this analysis and Collins(1995) are well matched with each other, even though their resultant flow fields show some differences. Because Yoon et al.[5] showed that the minimum moderator subcooling continued to decrease after 200 sec from a LOCA initiation, this transient calculation was performed until 200 sec.

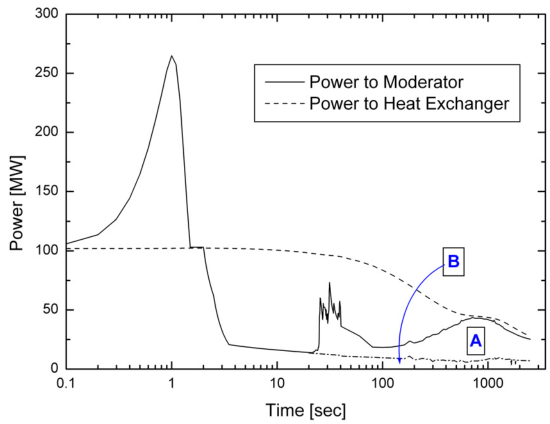

Figure 7 Total power to moderator and power to heat exchanger for 35% RIH with loss of ECC injection

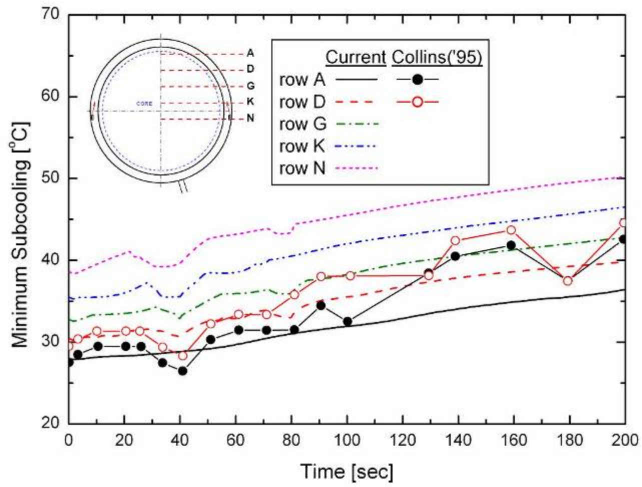

Figure 8 Minimum subcooling from CFX-10 moderator analysis for 35% RIH with loss of ECC injection

5. Conclusion

A CFD moderator analysis model was developed by using a coupled solver, which was found to be more effective and faster than a segregated solver. The computing time was reduced by more than 5 times. The developed model was verified and validated against experimental data, and used for the moderator analysis of Wolsong Units 2/3/4. From a transient calculation with constant operating conditions, fluctuating flow fields and temperatures were observed in the reflector region around a jet reversal. For a transient moderator analysis during LOCA events, FORTRAN subroutines were developed for the implementation of a time-dependent bundle heat load to the moderator. For a 35% RIH break with a loss of ECC injection, a transient moderator analysis was performed and the resultant minimum subcooling was estimated.

6. Acknowledgement

This study has been carried out as a part of the Development of Safety Issue Relevant Assessment System and Technology for CANDU NPP's program supported by Korea Ministry of Science & Technology.

7. Nomenclature

A = area [m^2]

L = length [m]

p = pressure [N/m^2]
pitch = pitch [m]
Re = Reynolds number
u = velocity components [m/sec]
U = velocity magnitude [m/sec]
x = coordinate component [m]
γ = porosity

μ = fluid viscosity [kg sec/m^2]
ρ = fluid density [kg/m^3]

Subscripts
A = area
tube = tube

8. References

[1] G Austman, J. Szymanski, M. Garceau and W.I. Midvidy, "Measuring Moderator Temperature in a CANDU Reactor," *6th Annual Conference of CNS*, Ottawa, Canada (1985)

[2] R.G. Huget, J.K. Szymanski, and W.I. Midvidy, "Status of Physical and Numerical Modelling of CANDU Moderator Circulation," *Proceedings of 10th Annual Conference of the Canadian Nuclear Society*, Ottawa (1989)

[3] R.G. Huget, J.K. Szymanski, and W.I. Midvidy, "Experimental and Numerical Modelling of Combined Forced and Free Convection in a Complex Geometry with Internal Heat Generation," *Proceedings of 9th International Heat Transfer Conference*, 3, 327 (1990)

[4] H.F. Khartabil, W.W. Inch, J. Szymanski, D. Novog, V. Tavasoli, and J. Mackinnon, Three-Dimensional Moderator Circulation Experimental Program for Validation of CFD Code MODTURC_CLAS, *21st CNS Nuclear Simulation Symposium*, Ottawa, Sept. 24-26 (2000)

[5] C. Yoon, B.W. Rhee, H.T. Kim, J.H. Park, and B.-J. Min, "Moderator Analysis of Wolsong Units 2/3/4 for the 35% Reactor Inlet Header Break with a Loss of Emergency Core Cooling Injection," *J. of Nuclear Science and Technology*, Vol. 43, No. 5 (2006)

[6] ANSYS CFX, Release 10.0: Manual, on-line Help form, ANSYS Inc. (2004)

[7] G.I. Hadaller, R.A. Fortman, J. Szymanski, W.I. Midvidy and D.J. Train, Frictional Pressure Drop for Staggered and In Line Tube Bank with Large Pitch to Diameter Ratio, *Preceedings of 17th CNS Conference*, Fredericton, New Brunswick, Canada (1996)

[8] L.N. Carlucci, V. Agranat, G.M. Waddington, H.F. Khartabil and J. Zhang, Validation of the MODTURC_CLAS Moderator Circulation Code for CANDU 9 Steady-State and Transient Conditions, *21st CNS Nuclear Simulation Symposium*, Ottawa, Sept. 24-26 (2000)